Optical Metamaterials for Photonics Applications

Derrick Langley[1], Ronald A. Coutu, Jr.[1], LaVern A. Starman[1], Stanley Rogers[2]

[1]Air Force Institute of Technology, Wright Patterson Air Force Base, OH 45433
[2]AFRL, Wright Patterson Air Force Base, OH 45433

Abstract

This paper discusses our investigation into artificial structures called metamaterials. Metamaterials make it possible to achieve electromagnetic properties not existing in nature. The investigation focuses on the modeling, fabrication and testing of metamaterials at optical frequencies. The main purpose of this research is to identify a method to fabricate the artificial structures. We identify limitations in the fabrication process which are used to build the metamaterials. Measured reflectance data from fabricated devices is then compared with modeled data to identify limitations affecting the "as-built" figure of merit (FOM). Understanding the parameters which limit the FOM will lead to device fabrication improvements and ultimately to components suitable for optical applications such as optical surveillance systems.

Keywords: optical, metamaterial, negative refractive index, fabrication, applications

1. BACKGROUND

Stemming from a landmark paper by V. G. Veselago, the race to create negative refractive material structures has been gaining momentum. Veselago [1] discusses the effect of the dielectric constant ε and the magnetic permeability μ. Both ε and μ are the fundamental characteristic quantities that determine the propagation of electromagnetic waves in matter. Both exist in the dispersion equation (1) which connects the frequency (ω) of a monochromatic wave and its wave vector k.

$$\left|\frac{\omega^2}{c^2}\varepsilon_{ij}\mu_{ij} - k^2\delta_{ij} + k_i k_j\right| = 0. \tag{1}$$

In Equation (1) above, c is the speed of light. The dispersion equation can be simplified for isotropic substances into Equation (2)

$$k^2 = \frac{\omega^2}{c^2}n^2. \tag{2}$$

By knowing that n^2 is the square of the index of refraction of the substance, we can replace n^2 with the permittivity and permeability through the use of Equation (3)

$$n^2 = \varepsilon\mu. \tag{3}$$

Veselago [1] presents a formal approach to achieving the electrodynamic properties of substances with negativity ε and negative μ. He explains how negative refractive materials can be physically realized by using materials such as pure ferromagnetic metals and semiconductors. Veselago further explains how to derive tensors of ε and μ which produce left-handed index of refraction. These left-handed substances, considered as gyrotropic materials or media, react to plasma in a specific or direction of propagation. The plasma's direction of propagation has to be along the magnetic field in order for negative values of ε and μ to be realized. Characteristics of gyrotropic substances consist of the following properties: The substance must contain sufficiently mobile carriers forming an electron-hole plasma and a system of interacting spins must exist which provide a large magnetic susceptibility [1]. Another issue pointed out by Veselago discusses frequency dispersion where he states that in the absence of frequency dispersion and/or absorption, the material cannot generate $\varepsilon < 0$ and $\mu < 0$, since under this condition, the total energy would be negative. Equation (4) provides the relation between energy W and the frequency dispersion.

Derrick Langley, Capt: E-mail: derrick.langley@afit.edu, Telephone: 1 937 255 3636
The views expressed in this article are those of the authors and do not reflect the official policy or position of the United States Air Force, Department of Defense, or the U.S. Government.

Adaptive Coded Aperture Imaging, Non-Imaging, and Unconventional Imaging Sensor Systems,
edited by Stanley Rogers, David P. Casasent, Jean J. Dolne, Thomas J. Karr, Victor L. Gamiz, Proc. of SPIE
Vol. 7468, 74680H · © 2009 SPIE · CCC code: 0277-786X/09/$18 · doi: 10.1117/12.828509

$$W = \frac{\delta(\varepsilon\omega)}{\delta\omega}E^2 + \frac{\delta(\mu\omega)}{\delta\omega}H^2. \quad (4)$$

where E is the electric field and H is the magnetic field. Using this relationship between energy and frequency dispersion, Veselago provides a detailed description on how to use this relationship to examine the effects of plasma propagation in metamaterial structures.

In recent years, numerous researchers published detailed results discussing novel structures with negative index of refraction. Several authors point out processes used to build and test the metamaterial structures based of Veselagos' modeling results [2, 3, 4, 5]. For example, an Infrared (IR) metamaterial structure was formed into a split ring resonator (SRR) by depositing a layer of gold on vanadium oxide. This SRR was fabricated on an alumina substrate which gave a dynamically tuned response over the far-IR frequency range. The swiss roll SRR created by J. B. Pendry, et al., is another metamaterial example which generates a wide range of permeabilities by using nonmagnetic thin sheets of metal sandwiched between dielectric materials. Initial results obtained from the swiss roll demonstrated a change in the permeability over a narrow frequency bandwidth. The focus areas for this study cover both the IR and optical spectral ranges; however, our main objective was to perform an iterative design implementation of these metamaterials to gain the necessary insight into the fundamental designs, fabrication and testing of these structures. Following the initial fabrication and testing, we will implement a design of experiments to optimize the metamaterial structures and testing procedures to maximize the level of negative permittivity μ.

2. IR STRUCTURE BACKGROUND

The SRR is commonly used to create IR metamaterials and typically composed of nonmagnetic metals like copper, gold, or silver which are positioned between dielectric materials to form the metamaterial structure [3]. The SRR can be scaled to sizes less than the incident wavelength while maintaining the functionality of a metamaterial structure. The diagonal ε and μ reflect the usual anisotropic properties of the metamaterial due to the orientation of the structure, for example, a periodic arrangement of metallic rods and rings [4]. By stacking the SRRs, the structure breaks the continuity along the vertical direction and the discrete rings arrayed in the vertical direction would mimic the action of a cylinder confining the magnetic flux inside [4]. By arranging the SRR in a plane, the structure responds to components of the excited magnetic field along the axis. Figure 1 shows isometric layout views of stacked SRRs based off the metallic rods and rings from Ramakishna. These layered metamaterial structures help define the resonant frequency response to in-plane electric fields and out-of-plane magnetic fields.

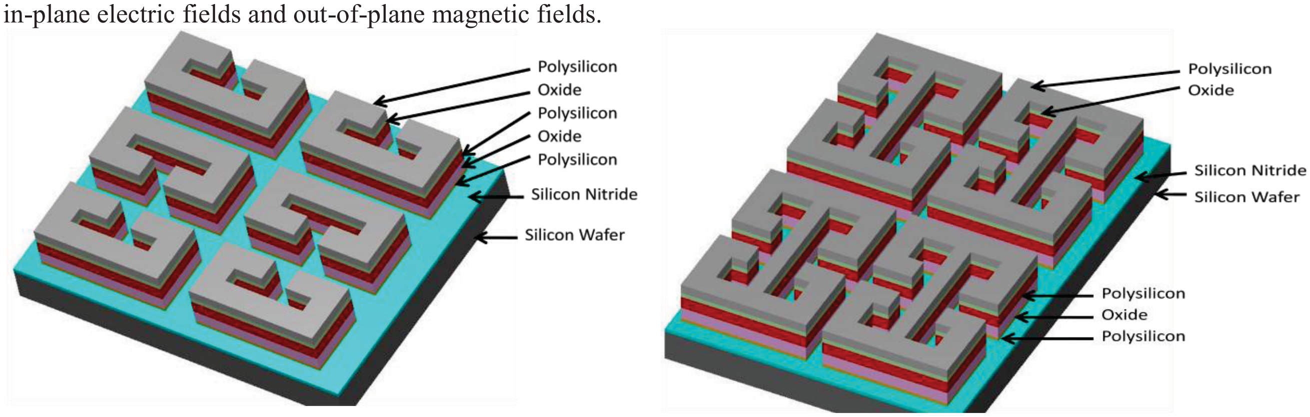

(a) (b)

Figure 1. IR Metamaterial Structures. (a) SRR layout with a periodicity of 20 μm and (b) SRR with rods with a periodicity of 34 μm .

OPTICAL STRUCTURE BACKGROUND

Optical metamaterials can be thought of as a scaling of IR structures to smaller dimensions which is necessary for features smaller than the incident wavelength. When comparing IR and optical metamaterials, slight structural changes are required between the two types of wavelengths. Fundamentally, both structural types consist of layers of nonmagnetic metal and dielectric material arranged in a periodic fashion to account for the electric and magnetic interaction. Both metamaterial types consist of layered materials which take advantage of the change in the refractive index. The main difference in the optical metamaterial structure is that the pattern takes on a different arrangement other than the SRR configuration. To date, researches achieved negative index on metamaterials at low wavelengths, publishing results at 1.8, 1.5, 1.4 0.813, and 0.772 µm [5]. For example, by modeling and fabricating an optical metamaterial structure, Chetter, et al, were able to demonstrate results for a material having simultaneously negative real parts of its effective ε and μ. This double negative-negative index material was achieved at 0.813 µm. With the same structure, Chetter et al., achieved the lowest negative index at 0.772 µm. The low negative index is used as a figure of merit (FOM) accepted by researchers for optimizing the performance of negative index material. The accepted FOM is the ratio of the real to the imaginary component of the refractive index. When the FOM is written in the following form, it gives an indication of why a double negative-negative index material is better than a single negative-negative index material.

$$\frac{-(|\mu|\varepsilon' + |\varepsilon|\mu')}{(|\mu|\varepsilon'' + |\varepsilon|\mu'')}. \tag{5}$$

In equation (5) ε' and μ' are the real parts of the effective permeability and permittivity, while ε" and μ" are the imaginary components.

Figure 2 shows the isometric view of optical structures used for this investigation. The layout of the structure helps to separate the magnetic and electric fields of an incident beam of light impinging on the metamaterial structure. An incident magnetic field is polarized along the plane shown by the direction of wider parallel strips between the etched stadium patterns. The magnetized strips from the different layers are coupled at the magnetic resonance thereby amplifying the magnetic field within the structure. For an optimized design, the magnetic resonance should be sufficiently strong in order to create negative values for the effective μ. The incident electric field alignment occurs along the narrow parallel strips which are perpendicular to the magnetic wider parallel strips. Overall, the electric field should not show any signs of diffraction because the structural dimensions are sub-wavelength when compared to the incident electric field. Through the use of the two isolated structures (wide and narrow strips) and understanding the interaction between the electric and magnetic fields, we can achieve $\varepsilon < 0$ and $\mu < 0$ through the tuning of the resonance frequencies within the overall metamaterial structure. For the optical fishnet, the thin metal film surrounded by the dielectric film provides the structure the ability to produce a negative index. Knowing the range of visible light covers the narrowband wavelength ranging from 0.390 to 0.780 µm and knowing the plasma frequencies of various metal films, one must consider these wavelengths and dimensions when designing optical fishnets structure for a sub-wavelength response. The following table lists metals and plasma frequencies for consideration as a thin film layer within the metamaterial structures.

Table 1. Plasma Frequency for metals.

Metal	Plasma Freq (eV)
Aluminum	15
Cesium	2.845
Gold	5.8
Lithium	6.6
Nickel	9.45
Palladium	7.7
Potassium	3.84
Silver	3.735

The plasma frequency is the natural frequency of oscillation within the metal at which free electrons and positive ions may be thought of as plasma. The plasma frequency serves as a critical value below which the index of refraction is complex and the penetrating waves drop off exponentially from the boundary [6]. The optical fishnet structural dimensions which consist of the film and dielectric thicknesses, widths and lengths, must be smaller than the wavelength of the incident radiation. Looking at the plasma frequency of a metal helps identify the metallic thin film to be used for our optical fishnet. For example, the structural units can range in sizes from $\lambda/5$, $\lambda/10$, to $\lambda/10000$, where λ is the optical wavelength. Using the plasma frequency for silver and the equation for photon absorption (Equation 6), we can equate the smallest wavelength at which silver does not absorb photons (0.332 µm).

$$\lambda = \frac{1.24}{E(eV)} \ (\mu m) \tag{6}$$

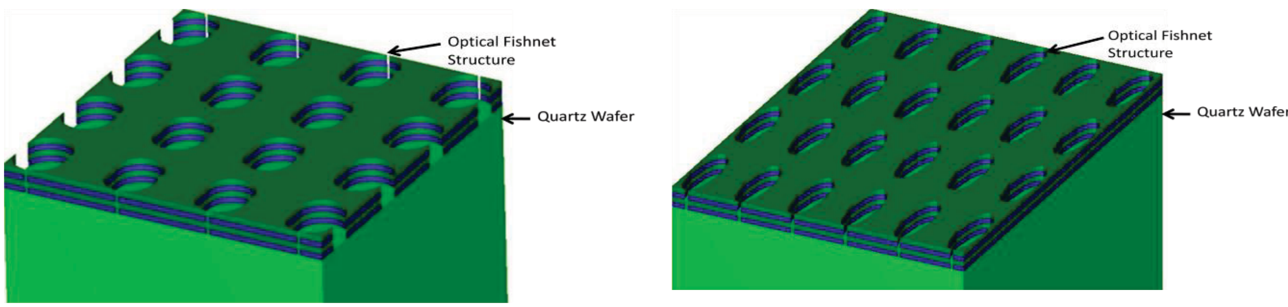

(a) (b)

Figure 2. Optical Fishnet Metamaterial structures, (a) Stadium design (b) Elliptical design

3. LAYOUT AND FABRICATION

Figures 1 and 2 are isometric views showing completed layout views of the infrared (IR) and optical metamaterial structures which were created by L-Edit©. This software package generates a circuit design layout which is used to simulate the metamaterial structural features. From the circuit design, L-Edit© generates mask layouts for design inspection prior to the physical patterning of the structures with photolithography masks and/or electron beam lithography.

The designed IR metamaterial structures were submitted to MEMSCAP Inc. for fabrication in a surface micromachining polysilicon process. The designs are based on split ring resonator structures which provide a proven method for IR metamaterial fabrication, and provides for an initial baseline for this investigation [2, 4]. Our structural designs consist of layers of polycrystalline silicon and silicon dioxide, which are commonly used in microelectronic device fabrication as structural and dielectric layers. Silicon nitride isolates the structure from a highly doped silicon substrate. The IR metamaterial structure in Figure 1(a) has a periodicity of 20 µm, while Figure 1(b) has a periodicity of 34 µm.

The optical structures were fabricated through an in-house effort at the Sensors Directoriate, Air Force Research Laboratory, Wright-Patterson AFB Ohio. The intial designs were based on a double negative index metamaterial demonstrated by Chettia, et al.[5]. Having a fundamental design to begin our development of the metamaterial structure reduced research and developmental time and gave a milestone for the in-house effort. The metamaterial structural layers are composed of multiple layers of Alumina (Al_2O_3) and Silver (Ag) with one layer of Galium doped Zinc Oxide (Ga-ZnO) which is used to bind the metamaterial layers to the substrate. Due to the nature of silver, the initial Al_2O_3 and Ga-ZnO layers were required to provide the adhesion of the metamaterial layers to the substrate. The Ga-ZnO layer was deposited by pulsed Laser deposition (PLD) which uses a laser to ablate the selected material target, creating a plasma plume of the material for deposition onto the desired substrate. In this case, the laser ablates the gallium and zinc-oxide targets in an atmosphere of oxygen. Following the initial PLD deposition layer, subsequence material layers (alumina and silver) were deposited by standard RF sputtering methods through the use of a Denton Discovery 22 Sputtering system. The final layer is a thin layer of Al_2O_3 which keeps the final (top layer) silver layer from deteriorating.

Fused silica was used for initial substrates to complete the etch studies for the metamaterial structural patterns. However, quartz substrates were used for the final etch studies because it offers better reliability for the processes used in the deposition of Ga-ZnO. One reason for this substrate selection is that quartz withstands the rapid temperature changes which occur during the PLD process; whereas, the fused silica wafers tend to crack or fracture because of the temperature shock during deposition. Another reason is optical transmission interference is reduced through the use of quartz substrates. Figure 2(a) shows the L-Edit 3-dimensional layout of the metamaterial based on Chettiar, et al. [5]. The stadium design is processed with electron-beam (E-beam) photolithography in order to pattern the structural dimensions below the wavelength of light. The final stadium dimensions have a length of 100 nm, a width of 150 nm, with a periodicity of 300 nm. In Figure 2(b), the elliptical pattern is modified from our initial stadium designs following initial research and investigations conducted by ourselves and others in the development of metamaterial sturctures.

To define the metamaterial structure, an etching process was developed to clear the alumina and silver in the stadium and elliptical areas. The 3-D layout in Figure 2 for the optical metamaterial graphically shows how ideal openings should appear after the etching process. In order to etch the materials, we developed a two step process to remove the alumina layer and then the thin silver film. An Ion Coupled Plasma (ICP) etcher was used to etch the stadium and elliptical patterns. The primary reason for using the ICP etcher is to control the etch profile and minimize the degree of undercutting in the stadium and eliptical structures. ICP etching also provides control over the etching process time, flow rates, and applied RF power. The first step of the etching process involves clearing the top layer of alumina with a boron trichloride ICP etch. This is followed by an argon ICP etch to clear away the oxide and silver layers. These two steps are repeated to clear multiple layers of alumina and silver. Shown in Figure 3, are scanning electron microscope (SEM) images illustrating the results of the etch process conducted on large open areas. The image in Figure 3(b) shows the aggressive nature of the etch process on the metamaterial sturcture at high RF bias. To minimize damage to the sidewall profiles, we recommend reducing the RF power during the two etching steps.

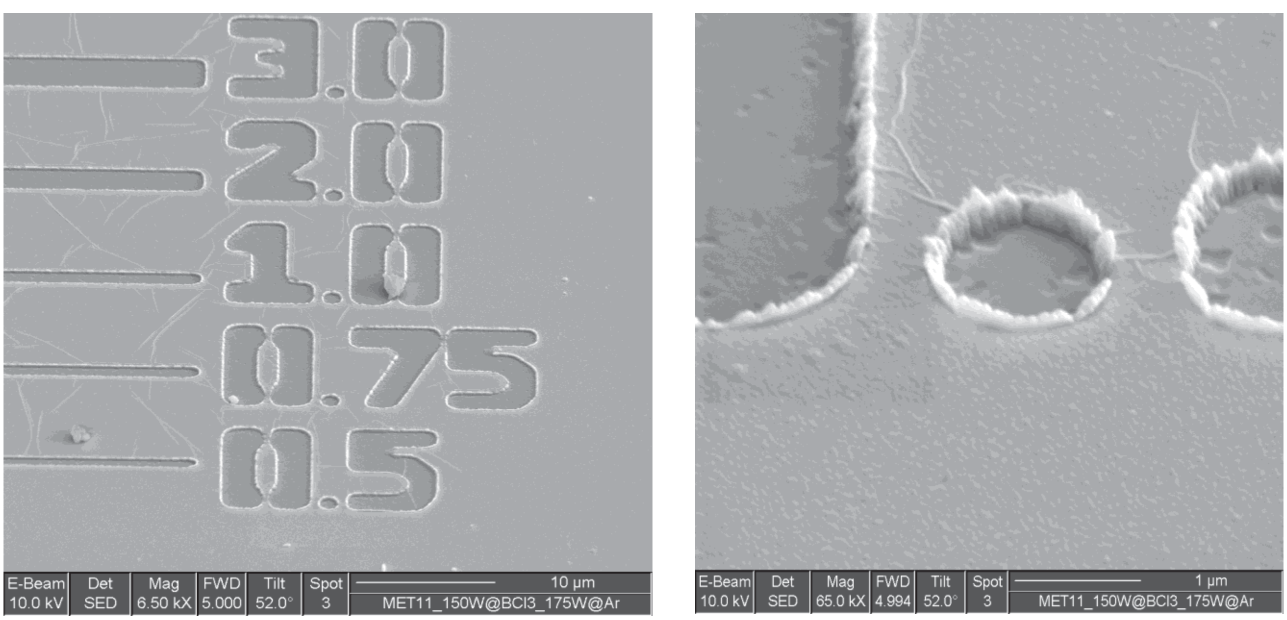

(a) (b)

Figure 3. Metamaterial layers etching, (a) View of large areas after etching. (b) Close up view following etching.

Figure 4 shows an SEM image of the initial fabrication results for the optical fishnet structure. The SEM image shown in Figure 4(a) is a 100 μm^2 optical fishnet. Figure 4(b) shows a close up view of the lower right hand corner of the optical fishnet. The E-beam photoresist used during the processing of the wafer was not removed prior to capturing these images. The dislocations in the resist are a result of rinsing the wafers with deionized water immediately after etching. Deionized water aides in the removal of loose resist which helps clear the etched areas following the etching process. By comparing the fabricated structure to Figure 2(a), the E-beam system creates an adequate profile with high resolution for the stadium and elliptical optical fishnet structures. The dimensions of the open patterns within the fabricated stadiums are 100 nm x 150 nm (±20 nm) with a periodicity of 300 nm (±20 nm). To further improve the structure, investigations are being conducted into the ICP etching process by using a lower RF bias with shorter etch times for both material layers.

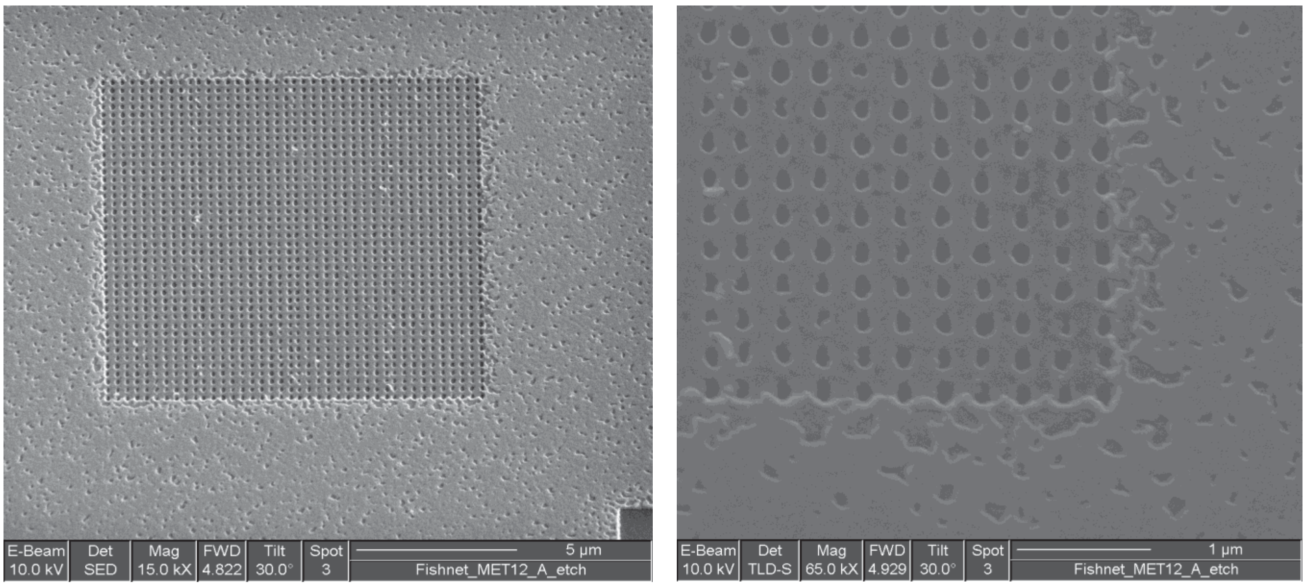

(a) (b)

Figure 4. SEM Images of Optical Fishnet Structures a) The 100 μm^2 optical fishnet area. b) A view of the lower right hand corner area of the optical fishnet

4. FABRICATION PROCESS CONTROL EXPERIMENTAL RESULTS

While processing the optical metamaterial structural layers, various samples were tested for layer thickness and optical properties. A spectroscopic ellipsometer, which has a spectral range of 0.6 to 4.7 eV, was used to test the structural layers. The ellipsometer was located in a class 100 cleanroom which reduced the possibility of surface contamination from debris and improper handling of the samples outside the facility. The ellipsometer uses phase modulated ellipsometry to obtain measurements based on birefringement tuner controlled polarization. The raw data (ψ, Δ, Is, Ic) is subsequently analyzed with the self-contained DeltaPsi2 (DP2) software package, which employs non-linear regression to extract layer thickness and optical constants. Generally, spectroscopic ellipsometers can obtain the following material properties: 1) film thickness, 2) refractive index, 3) extinction coefficients, 4) surface roughness, 5) interfacial mixing, 6) material composition, 7) crystallinity, 8) anisotropy, 9) depolarization, and 10) uniformity (depth and surface).

The metamaterial layers are tested over the IR (0.6 – 1.50 eV), visible (1.5 – 3.5 eV) and near UV (3.5 – 4.75 eV) spectral ranges and at three different angles of incidence (50, 60, and 70 degrees). The ellipsometric data is analyzed using DP2 in two steps: Step 1 uses a standard Drude model for the optical constants in the spectral range of 1.5 to 3.5 eV, where repeatable and reliable determination of the thickness and the optical constants are obtained. Step 2 then assumes the thickness determined in Step 1, and a uses Lorentz model for the optical constants in the spectral range of 3.5 to 4.75 eV to complete the characterization of the metamaterial over the full spectral range. Figure 5 shows the graphical results for each of the two data analysis steps for silver deposited on silicon. The figures show the ellipsometric variables (*Is, Ic*) versus change in photon energy (eV), where the dotted lines are the measured raw data and the smooth lines are the fits from the selected optical models discussed above.

With the Denton 22 sputtering system, we deposited silver layers onto silicon wafers at two thicknesses and compared the values. Using the spectroscopic ellipsometer and a step height profilometer, the silver layer thicknesses of 0.25 and 0.50 µm were tested and verified by comparing it to the expected values for the sputtering deposition. Both layer thicknesses agreed as expected.

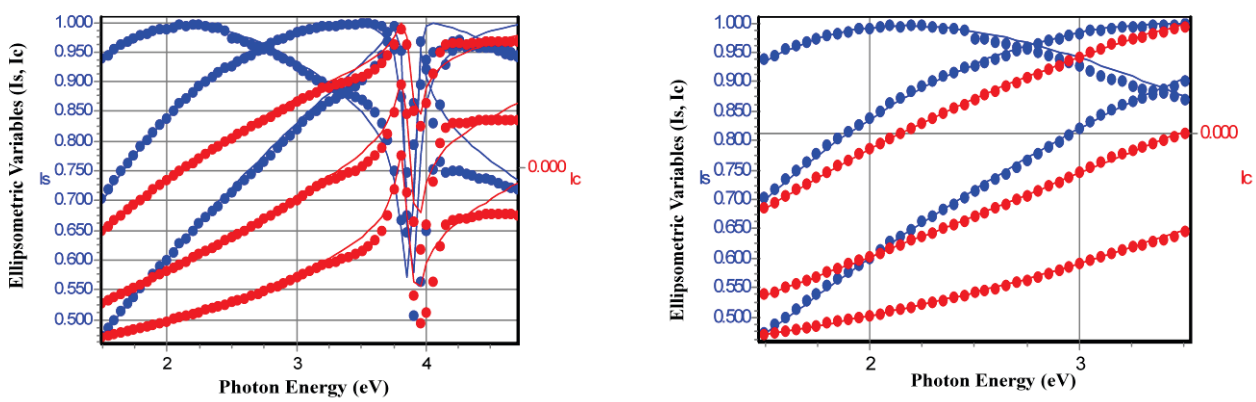

(a) (b)

Figure 5. a) Ellipsometric variables (IS, Ic) versus photon energy over the full spectral range. b) Ellipsometric variables (Is, Ic) versus photon energy in the NIR and visible region.

5. APPLICATIONS

A potential outcome of the research into metamaterial structures is the development of technologies in support of surveillance applications. One of the major hindrances to current surveillance systems is the fill factor for image collection. Fill factor is described by the amount of scene or image captured by optical systems during one observation. By incorporating metamaterial structures into future systems, we hope to make improvements beyond the current fill factor for modern systems.

Another potential advantage gained by our investigation into metamaterial structures will be the reduction of size, weight, and power for IR and optical systems. Having the ability to reduce the size and weight of surveillance platforms will help reduce costs for implementing systems into larger programs. Reducing power requirements will permit easier system integration onto platforms having limited available power.

If the investigation into metamaterials for optical applications generate promising results, two dimensional active (2D active) spatial light modulation will be studied by employing metamaterial structures. By incorporating the metamaterial structures into spatial light modulators, we hope to provide future surveillance system with higher fill factors and 2D active controls.

Two application developments currently beyond reach with today's metamaterial's technology are prism-like structures and inertia-less micro-shutter array structures. The prism-like structure can be described as a flat planar structure with similar characteristics, for an impinging light, as a triangular prism. Using a varying periodic array of metamaterial structures, we will investigate this triangular prism-like phenomenology. The inertia-less micro-shutter structure is envisioned as a system that can block or refract light from a detector without moving parts. The theory behind metamaterial structures gives rise to this concept because of the change in reflectance and transmission of light through a bi-stable structure.

6. CONCLUSION

Designing metamaterial structures that work at IR and optical wavelengths help build an understanding of the modeling and fabrication processes involved. The initial designs and fabrication show promising results that can lead to operational metamaterials at lower wavelengths. We are continuously making improvements to the various process steps used to create the structures. The testing and fabrication improvements along with the application and system integration concepts described earlier will be the future focus of our metamaterial design efforts.

Disclaimer: The views expressed in this article are those of the author and do not reflect the official policy or position of the United States Air Force, Department of Defense, or the U.S. Government.

REFERENCES

[1] Veselago, V.G., "The Electrodynamics of substances with simultaneously Negative Values of ε and μ," Uspekhi Fizicheskikh Nauk, 10(4), 509-514 (1968).
[2] Driscoll, T., Palit, S., Qazilbash, M. M., Brehm, M., Keilmann, F., Chae, B-G, Yun, S-J, Kim, H-T, Cho, S. Y., Jokerst, N. M, Smith, D. R., and Basov, D. N., "Dynamic tuning of an infrared hybrid-metamaterial resonance using vanadium dioxide," Applied Physics Letters 93, 024101 (2008).
[3] Pendry, J. B., Holden, A. J., Robbins, D. J., and Stewart, W. J., "Magnetism from Conductors and Enhanced Nonlinear Phenomena," IEEE Transactions on Microwave Theory and Techniques, 47(11), 2075-2084 (1999).
[4] Ramakishna, S. A, Grzegorczyk, T. M., [Physics and Application of Negative Refractive Index Materials], CRC Press, Bellingham, (2009).
[5] Chettiar, U. K., Kildishev, A. V., Yuan, H. –K., Cai, W., Xiao, S., Drachev, V. P., and Shalaev, V. M., "Dual-Band Negative Index Metamaterial: Double-Negative at 813 nm and Single-Negative at 772 nm," Optics Letters 32(12), 1671-1673 (2007)
[6] Hecht, E., [Optics 4th Ed.], Pearson Addison Wesley, San Francisco CA, (2002).